



Deep learning based optimal energy management framework for community energy storage system[☆]

Md. Morshed Alam, Yeong Min Jang^{*}

Department of Electronics Engineering, Kookmin University, Seoul 02707, Republic of Korea

Received 29 October 2021; received in revised form 19 February 2022; accepted 17 May 2022

Available online xxx

Abstract

This paper proposes a deep learning-based integrated framework for multiple cooperative households to achieve optimal energy distribution. The corresponding energy generation and consumption problems are formulated by a long short-term memory algorithm is combined with an optimization algorithm to produce an optimal solution. In this study, a PV-community energy storage system (CESS) integrated is considered where the scheduling decision of the CESS and utility grid can be subsequently achieved through formulated constraints. The test results demonstrate the efficacy and robustness of the proposed system that achieves superior performance on effective renewable energy usages of maximum 31.74% in a home environment.

© 2022 The Author(s). Published by Elsevier B.V. on behalf of The Korean Institute of Communications and Information Sciences. This is an open access article under the CC BY-NC-ND license (<http://creativecommons.org/licenses/by-nc-nd/4.0/>).

Keywords: Energy storage system; Long short term memory; Optimization algorithm; Home energy management system

1. Introduction

The need for electricity has risen significantly in various areas because of the huge development of businesses, factories, and population growth. As a result, the integration of electrical components in a wide range of applications expand rising energy demands. According to the International Energy Agency, global electric power consumption will increase at a rate of 2.1% per year through 2040 (IEA). Furthermore, global energy consumption is expected to rise from 19% in 2018 to 24% in 2040 [1]. The rise in energy demand over the last several decades can also be attributed to consumers' modernistic lives.

As more energy storage is installed throughout the world, especially in household loads-renewable energy (RE) integrated system, community energy storage system (CESS) has increased in popularity. As a result, CESS has been installed all over the world, particularly in Australia, the Netherlands,

and the United States [2,3]. However, as the energy system's infrastructure improves, users can optimize their real-time energy consumption by combining artificial intelligence with home energy management systems (HEMS). If CESS is included in the system, such an optimization process will be more effective and reliable. CESS generates collective socio-economic benefits based on its dependencies and constraints, such as self-consumption and higher renewable resources integration, reduced reliance on fossil fuels, lower electricity bills, revenue generation via various energy services, and increased local economy [4].

1.1. Related work

Several researchers have proposed different methodologies and schemes for controlling and evaluating shared energy storage systems. Wang et al. [5] proposed an ESS operation management approach that takes into account electricity pricing and power demand thresholds, with customers and the network regulating energy storage capacity. Sardi et al. [6] developed a shared energy storage control mechanism based on charging and discharging substation power thresholds by considering some benefits such as energy arbitrage, peaking power generation, and energy loss reduction. In [7], the authors developed a charging envelope-based control strategy based

[☆] This work was partly supported by the Technology Development Program of MSS (S3098815) and the MSIT (Ministry of Science and ICT), Korea, under the ITRC (Information Technology Research Center) support program (IITP-2022-2018-0-01396) supervised by the IITP (Institute for Information & Communications Technology Planning & Evaluation).

^{*} Corresponding author.

E-mail addresses: mmorshed@ieee.org (M.M. Alam), yjang@kookmin.ac.kr (Y.M. Jang).

Peer review under responsibility of The Korean Institute of Communications and Information Sciences (KICS).

<https://doi.org/10.1016/j.ict.2022.05.007>

2405-9595/© 2022 The Author(s). Published by Elsevier B.V. on behalf of The Korean Institute of Communications and Information Sciences. This is an open access article under the CC BY-NC-ND license (<http://creativecommons.org/licenses/by-nc-nd/4.0/>).

on the state of charge (SOC), charging and discharging period constraints, and distribution network operators. In shared ESS, an energy exchange scheme based on dynamic programming is used to exchange energy between ESS operations and individual ESS units of residential users [8]. Moreover, residential consumers can purchase or sell their allotted shared energy storage capacity, charging–discharging timetable, and the amount of charging and discharging power for the shared ESS [9,10]. In [11], Carli et al. proposed a method for determining the best charging and discharging profiles for a shared battery energy storage system via energy exchanges with the grid and management of controlled loads. In an article [12], and energy sharing platform is created to effectively exchange power between hybrid ESS and utility grid based on the different sizes of thermal and gas systems, improving system reliability and reducing the fluctuation of RE resources. In [13], the authors proposed stochastic model predictive control based robust optimal scheduling algorithm for minimizing the community electricity cost through controllable and non-controllable loads in the grid-connected energy community. In addition, two stages stochastic programming is used for forecasting uncertainties and model predictive control strategy have been developed for micro-grid for reducing uncertainties issues by considering battery, distributed generation, PV, and wind [14].

1.2. Contributions

In [15], the energy management scheme for ESS by two-stages management (i.e., hourly and minute-level operation strategies) and predictable model have been proposed while the scheduling and optimization of CESS along with multiple households are not taken into consideration. In [16,17], the authors investigate energy management schemes under uncertain environments and promote curtailing of energy usage and proposes a scheduling scheme for minimizing the cost of microgrid framework. Moreover, a PV-ESS (i.e., PV system connected with energy storage system) integrated system has adopted an effective scheduling technique in a domestic residence for minimizing energy expense [18–20]. The authors of those publications concentrate on charging and discharging times without taking into account expected PV power output and home energy consumption. As a result, rather than charging, the ESS releases stored energy during PV production. Furthermore, because of a lack of charge in the ESS, the appliances draw electricity from the grid at times of high demand. Although the previous research is comparable to this research, the goal of this paper is to design a control scheme for the shared ESS by compromising maximum PV generation and ESS stored energy usage within constraints. In contrast to previous studies, the optimal energy management methodology proposed in this article takes into account forecasted daily energy consumption as well as a PV generation profile that reflects the use of renewable resources. Multiple households connected with PV integrated CESS are contemplated, which means that the CESS will distribute power among them by influencing their requirement as well as PV generation profile.

Therefore, the contributions of this include the following:

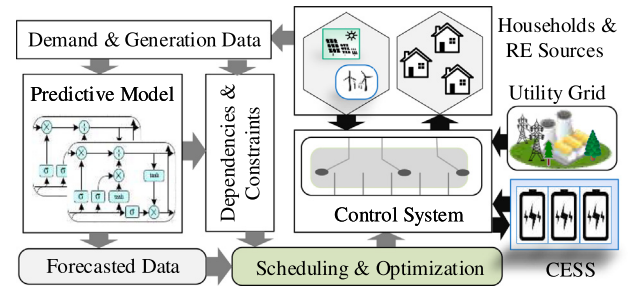


Fig. 1. Proposed shared energy management system framework. Black and gray arrows represent the flow of energy and information, respectively.

- We propose a novel HEM model based on a predictive machine learning algorithm combined with an energy sharing optimization algorithm within a data-driven framework. The test results indicate a promising performance in terms of PV generation and demand daily.
- The conventional schemes are only based on an optimization algorithm with a certain number of constraints. However, these assumptions are inconsistent and less effective since the ahead generation and consumption are vague. In contrast, our proposed data-driven HEM model can predict future uncertainties using an LSTM-based predictive model and make the best scheduling decision using an optimization algorithm.
- In dealing with different types of consumption profiles in the residential house, a multi-objective-based optimization algorithm is designed to tackle the scheduling problem involved with CESS.

The remainder of this paper is structured as follows. Section 2 describes the mathematical model for energy consumption, PV generation, and CESS. Section 3 presents test results to demonstrate the efficacy of our proposed scheme. Section 4 brings the manuscript to a conclusion.

2. Methodology

This study considers a scenario where a PV-equipped energy storage system is shared by multiple households for utilizing the stored energy. The framework of the proposed system is shown in Fig. 1. In this case, the consumer's energy demand is met through the utility grid and stored energy supply together. The CESS is charged during PV power generation and discharged based on the needs of the user for the rest of the time. In [21], the authors focus on the scheduling periods of CESS for an optimum solution where multiple households are considered. In this study, the system is used to design and analyze a data-driven optimal energy sharing algorithm.

2.1. System modeling

The process of data-driven optimal energy sharing algorithm is described briefly below:

Step 1: Firstly, collect the required data of households and PV system according to the prediction target. Then clean and

Table 1

Hyper-parameters for LSTM model.

Hyper-parameter	Value
Model nodes	64
Optimizer, Loss function	adam, MSE
Number of epochs, Batch size	50, 16
Train, Validation, and Test data size	66%, 16%, 18%

prepare the data for the predictive model. In addition, scaling the data for better accuracy.

Step 2: Split the dataset into train and test by adjusting the prediction objectives. Then, create data set according to the model requirements.

Step 3: Create the LSTM model and define all parameters inside the model. Evaluate the performance parameters.

Step 4: Use the forecasted result and required constraints in scheduling algorithm for determining the charging and discharging periods of the CESS.

Step 5: Finally, minimize the objective function by considering scheduling periods and necessary constraints.

2.2. Long short term memory

A long short-term memory (LSTM) cell unit is a modified version of a recurrent neural network that consists of an input, a forget, and an output gate [22]. Eqs. (1)–(6) present the operations of the LSTM network, where W and b are weight matrix and bias vectors, respectively. The three gates operate using the mechanism of a sigmoid function σ , which regulates the cell state (C_t). The forget gate f_t controls the cell state via an output number ranging from 0 (discard information) to 1 (keep information). By combining with the hidden state h_t , the input gate i_t decides to keep the information in the cell state. The old cell state C_{t-1} gets updated into C_t by Eq. (3). Eq. (4) presents potential vector \bar{C}_t ranging from 0 to 1 which is used for determining cell state, where \tanh is the hyperbolic tangent function. Finally, the output o_t of the output gate is formulated in Eq. (5).

$$f_t = \sigma(W_f[h_{t-1}, x_t] + b_f) \quad (1)$$

$$i_t = \sigma(W_i[h_{t-1}, x_t] + b_i) \quad (2)$$

$$C_t = f_t * C_{t-1} + (1 - f_t) * \bar{C}_t \quad (3)$$

$$\bar{C}_t = \tanh(W_c[h_{t-1}, x_t] + b_c) \quad (4)$$

$$o_t = \sigma(W_o[C_t, h_{t-1}, x_t] + b_o) \quad (5)$$

$$h_t = o_t \cdot \tanh(C_t) \quad (6)$$

Consider the input data and output data of the LSTM model are \bar{X} and \bar{Y} . Therefore, the input and output relation of the proposed model can be expressed as follows:

$$[\bar{Y}_t] = LSTM([\bar{X}_{t-S_t}, \dots, \bar{X}_{t-2}, \bar{X}_{t-1}]), \quad \forall t \in [t_{st}, t_{ed}] \quad (7)$$

where S_t is defined as the window size. In the proposed model, we have used window size = 96 (i.e., a single day) due to having 15 min time intervals data. The train, validation, and test data size are 66%, 16%, and 18%, respectively. Accordingly, the train and test input data shapes are (11404, 96, 1) and (3110, 1). Therefore, the LSTM model is designed through the adjustment of the parameters of the networks. In the model, the “adam” optimizer and “mean squared error (MSE)” loss function is used while the learning rate of the optimizer is .001. The mean The parameters of the model are presented in Table 1. The forecasting of energy consumption and PV generation data is discussed in Sections 2.3 and 2.4.

2.3. Scenario of household demand

The mathematical model is formulated to determine each individual consumer’s constraints and dependencies based on their daily electricity demand profile. Because the constraints and assumptions are derived from the predicted model, a household’s actual demands (D) are defined as $E_{D,t}^H(t)$. If the house (H) has $N \in Z$ appliances (A_i), the total energy (E) at time t can be expressed as follows:

$$E_{D,t}^H(t) = \sum_{i=1}^N E_{D,t}^{H,A_i}(t) \quad (8)$$

Similarly, for house no. 1 (H_1), house no. 2 (H_2), and house no. 3 (H_3), we may determine $E_{D,t}^{H_1}(t)$, $E_{D,t}^{H_2}(t)$, and $E_{D,t}^{H_3}(t)$. Let’s consider the household’s predicted demands at time t is $E_{FD,t}^H(t)$. The input ($E_{D,t}^H$) and output ($E_{FD,t}^H$) of the predictive model can be presented as follows:

$$[E_{FD,t}^H] = LSTM([E_{D,t-S_t}^H, \dots, E_{D,t-2}^H, E_{D,t-1}^H]) \quad (9)$$

According to the above equation, the forecasted demand of two consecutive days for H_1 , H_2 , and H_3 are determined. The total energy usage from t to the current day (t_{ed}) is calculated as follows:

$$E_{FD,[t,t_{ed}]}^H(t) = \sum_{j=1}^e \sum_{i=1}^N E_{FD,\tau}^{H,A_i}(j\tau) - \sum_{j=1}^k \sum_{i=1}^N E_{D,t}^{H,A_i}(t - j\tau) \quad (10)$$

$$t \in [0, 24], e = \frac{24}{\tau}, \text{ and } k = (\frac{t}{\tau} - 1) \text{ where, } t = \text{hour}$$

$$t \in [0, 1440], e = \frac{1440}{\tau}, \text{ and, } k = (\frac{t}{\tau} - 1) \text{ where } t = \text{minute}$$

The static and dynamic forecasted average power usage during 24-hours can be formulated as follows:

$$E_{FD,[t_{st},t_{ed}]}^{H,Avg} = \frac{\sum_{i=1}^n \sum_{j=1}^e E_{\tau,d}^{H,A_i}(j\tau)}{e} \quad (11)$$

$$E_{FD,[t,t_{ed}]}^{H,Avg}(t) = \frac{E_{FD,[t,t_{ed}]}^H(t)}{e - k} \quad (12)$$

Similarly, the average power of single day for three households can be defined as $E_{FD,[t_{st},t_{ed}]}^{H_1,Avg}$, $E_{FD,[t_{st},t_{ed}]}^{H_2,Avg}$, and $E_{FD,[t_{st},t_{ed}]}^{H_3,Avg}$. Therefore, the dynamic average power for three households can be expressed as $E_{FD,[t,t_{ed}]}^{H_1,Avg}(t)$, $E_{FD,[t,t_{ed}]}^{H_2,Avg}(t)$, and $E_{FD,[t,t_{ed}]}^{H_3,Avg}(t)$. The minimum and maximum demand of the households

are being determined from the historic data of the particular household. The minimum and maximum allowance of demand of any house can be expressed as $E_{D,t}^{H,min}$ and $E_{D,t}^{H,max}$. The power consumption allowance can be expressed as follows:

$$E_{D,t}^{H_1,min} \leq E_{D,t}^{H_1}(t) \leq E_{D,t}^{H_1,max} \quad (13)$$

$$E_{D,t}^{H_2,min} \leq E_{D,t}^{H_2}(t) \leq E_{D,t}^{H_2,max} \quad (14)$$

$$E_{D,t}^{H_3,min} \leq E_{D,t}^{H_3}(t) \leq E_{D,t}^{H_3,max} \quad (15)$$

2.4. Scenario of PV power

The proposed scheme includes a single PV-generating system, several houses, and CESS integration. PV power generation and forecasted PV power generation, denoted as $P_{Gen,t}^{PV}$ and $P_{FGen,t}^{PV}(t)$, can be used to represent PV power limitations and dependencies. The total energy production at time t can be expressed as follows:

$$P_{Gen,t}^{PV} = \sum_{i=1}^N P_{Gen,t}^{PV,M_i}(t) * \xi_{PV}^{M_i}(t) \quad (16)$$

where $\xi_{PV}^{M_i}(t) \in [1, 0]$ specifies the PV module's operational state at time t . The duration between starting and ending generation time describes as $t \in [t_{st}, t_{ed}]$, where $j = 0$ at the starting period and $p = t_{ed}/\tau$ and $q = \frac{(t-t_{st})}{\tau}$ at the ending period. Let us consider the forecasted generation at time t is $P_{FGen,t}^{PV}$, it can be formulated as follows:

$$[P_{FGen,t}^{PV}] = LSTM([P_{Gen,t-S_1}^{PV}, \dots, P_{Gen,t-2}^{PV}, P_{Gen,t-1}^{PV}]) \quad (17)$$

According to the above equation, the forecasted generation of two consecutive days is determined.

$$P_{FGen,[t_{st},t_{ed}]}^{PV}(t) = \sum_{j=0}^p \sum_{i=1}^N P_{FGen,t+\tau}^{PV,M_i}(t_{st} + j\tau) * \xi_{PV}^{M_i}(t) \quad (18)$$

$$P_{FGen,[t_{st},t_{ed}]}^{PV,Avg}(t) = \frac{P_{FGen,[t_{st},t_{ed}]}^{PV}(t)}{p} \quad (19)$$

$$P_{FGen,[t,t_{ed}]}^{PV}(t) = \sum_{j=0}^p \sum_{i=1}^N P_{FGen,t}^{PV,M_i}(t_{st} + j\tau) * \xi_{M_i}^{PV}(t) - \sum_{j=0}^q \sum_{i=1}^N P_{FGen,t+\tau}^{PV,M_i}(t - j\tau) * \xi_{M_i}^{PV}(t) \quad (20)$$

$$P_{FGen,[t,t_{ed}]}^{PV,Avg}(t) = \frac{P_{FGen,[t,t_{ed}]}^{PV}(t)}{p - q} \quad (21)$$

Eq. (18) describes the amount of power generated in a single day. Eq. (19) calculates the PV panel's expected average generation. Eqs. (20) and (21) can be used to calculate the total and average forecasted power from t to t_{ed} periods, respectively.

2.5. Scenario of CESS power

The following mathematical model is formulated for finding constraints and dependencies of CESS by which the optimal charging and discharging operations can be designed. The constraints used for charging and discharging of the ESS must

be governed by PV power generation and electricity demand characteristics.

$$P_{Gen,th}^{PV} \leq P_{Gen,t}^{PV}(t), S_{t,c}^{CESS}, t \in [t_{st}, t_{ed}], \quad (22)$$

$$SOC_{t,max}^{CESS} > SOC_t^{CESS}(t), S_{t,c}^{CESS}, t \in [t_{st}, t_{ed}] \quad (23)$$

$$SOC_{t,min}^{CESS} < SOC_t^{CESS}(t) \leq SOC_{t,max}^{CESS}, S_{t,d}^{CESS} \quad (24)$$

where $S_{t,c}^{CESS}$ are binary variables that represent the ESS's charging/discharging status. The ESS's minimal and maximum states of charge were represented by the variables $SOC_{t,min}^{CESS}(t)$ and $SOC_{t,max}^{CESS}$. Constraint Eq. (22) permits the CESS to charge itself, while constraint Eq. (23) prevents it from overcharging. The threshold value of PV power generated that allows storage to be charged is defined as $P_{Gen,th}$. Constraint Eq. (24) represents the CESS discharging allowance to households.

2.6. Mathematical formulation for optimal solution

The following constraints and mathematical formulation are developed for obtaining optimal solution for each household by considering the principle of CESS. According to the principle, the CESS can supply energy to two different households simultaneously based on demanded load and discharging allowance. We consider the charging period during PV generation and the rest of the period will be treated as discharging period depends on the stored energy because the charging and discharging processes in energy storage are not feasible at the same time. Let's consider the initial charge amount of the battery is $E_t^{CESS}(t-1) = E_{ini}^{CESS}$, the amount of the stored energy in the ESS can be expressed as follows:

$$E_t^{CESS}(t) = P_{Gen,t}^{PV}(t) + E_{t-1}^{CESS}(t-1) \quad (25)$$

Because of the frequent changes in demand of the consumer, the requirements of receiving energy will be changed. Consequently, there is a possibility of mismatching discharging time. The forecasted dynamic average value of the load profile was taken into account for formulating the period of each consumer as well as to avoid the uncertainty of the scheduling period. The scheduling constraints for discharging CESS are as follows:

$$E_{FD,[t,t_{ed}]}^{H_1,Avg}(t) \geq E_{FD,[t,t_{ed}]}^{H_2,Avg}(t) \quad (26)$$

$$E_{FD,[t,t_{ed}]}^{H_1,Avg}(t) < E_{FD,[t,t_{ed}]}^{H_2,Avg}(t) \quad (27)$$

$$E_{FD,[t,t_{ed}]}^{H_1,Avg}(t) \geq E_{FD,[t,t_{ed}]}^{H_3,Avg}(t) \quad (28)$$

$$E_{FD,[t,t_{ed}]}^{H_1,Avg}(t) < E_{FD,[t,t_{ed}]}^{H_3,Avg}(t) \quad (29)$$

$$E_{FD,[t,t_{ed}]}^{H_2,Avg}(t) \geq E_{FD,[t,t_{ed}]}^{H_1,Avg}(t) \quad (30)$$

$$E_{FD,[t,t_{ed}]}^{H_2,Avg}(t) < E_{FD,[t,t_{ed}]}^{H_1,Avg}(t) \quad (31)$$

$$E_{FD,[t,t_{ed}]}^{H_2,Avg}(t) \geq E_{FD,[t,t_{ed}]}^{H_3,Avg}(t) \quad (32)$$

$$E_{FD,[t,t_{ed}]}^{H_2,Avg}(t) < E_{FD,[t,t_{ed}]}^{H_3,Avg}(t) \quad (33)$$

$$E_{FD,[t,t_{ed}]}^{H_3,Avg}(t) \geq E_{FD,[t,t_{ed}]}^{H_1,Avg}(t) \quad (34)$$

$$E_{FD,[t_{st},t_{ed}]}^{H_3,Avg}(t) < E_{FD,[t_{st},t_{ed}]}^{H_1,Avg}(t) \quad (35)$$

Algorithm 1 Optimal energy sharing algorithm

Input:

Forecasted data, charging, and discharging constraints

Output:

Scheduling period and discharge allowance volume

```

1: begin
2: ask  $E_{G,th}^{PV}$ ,  $SOC_{t,min}^{CESS}$  and  $SOC_{t,max}^{CESS}$  of ESS
3: Determine  $SOC_t^{CESS}(t)$  at the beginning
4: for every household and PV system do
5:   for every certain interval do
6:     Compute Eq. (8), Eqs. (10)–(12) and Eqs. (18)–(21)
7:   end for
8: end for
9: go to Algorithm 2
10: while every certain interval do
11:   for every household do
12:     for every certain interval do
13:       Compute Eq. (41) and Eq. (43)
14:     end for
15:   end for
16:   for every certain interval do
17:     Determine sum of discharge amount
18:   end for
19:   Minimize Eq. (42)
20: end while
21: end

```

$$E_{FD,[t,t_{ed}]}^{H_3,Avg}(t) \geq E_{FD,[t,t_{ed}]}^{H_2,Avg}(t) \quad (36)$$

$$E_{FD,[t,t_{ed}]}^{H_3,Avg}(t) < E_{FD,[t,t_{ed}]}^{H_2,Avg}(t) \quad (37)$$

A combination of constraint Eqs. (26)–(37) allows each consumer to receive energy from the CESS. The maximum discharging allowance of each consumer differs because of the different profiles of load. Constraint Eqs. (38)–(40) allow the maximum limits of taking power from the CESS. We considered each consumer's maximum limit to be its maximum demand. The set of discharged energy for households is defined as $\{E_{Dis,t}^{H_1}(t), E_{Dis,t}^{H_2}(t), E_{Dis,t}^{H_3}(t)\} \in E_{Dis,t}^{H_h}(t), h \in N$. The following is a description of the maximum discharging allowance:

$$0 \leq E_t^{Dis,H_1}(t) \leq E_{D,t}^{H_1,max} \quad (38)$$

$$0 \leq E_t^{Dis,H_2}(t) \leq E_{D,t}^{H_2,max} \quad (39)$$

$$0 \leq E_t^{Dis,H_3}(t) \leq E_{D,t}^{H_3,max} \quad (40)$$

The total discharged energy of individual consumer will be varied after taking into consideration the level state of charge (SOC) of CESS. The discharging amount will be varied concerning $w = \frac{1}{\alpha}$, where iteration number is defined by α . Therefore, the discharging allowance can be expressed as follows:

$$E_t^{Dis,H_h}(t) = E_{D,t}^{H_h}(t) - w * E_{D,t}^{H_h,min}(t) \quad (41)$$

Algorithm 2 Scheduling algorithm

```

1: for every certain interval do
2:   if Eq. (22) and Eq.(23) then
3:     Only charging period is available
4:     Compute  $E_t^{CESS}(t)$  by Eq. (25)
5:   else if Eq. (24) then
6:     if Eq. (26) & Eq. (28) then
7:        $H_1 \leftarrow 1$  {1 means discharge period}
8:     if Eq. (33) then
9:        $H_3 \leftarrow 1$  and  $H_2 \leftarrow 0$  {1 means non-discharge period}
10:    else if Eq. (37) then
11:       $H_2 \leftarrow 1$  and  $H_1 \leftarrow 0$ 
12:    end if
13:    else if Eq. (30) & Eq. (32) then
14:       $H_2 \leftarrow 1$ 
15:    if Eq. (29) then
16:       $H_3 \leftarrow 1$  and  $H_1 \leftarrow 0$ 
17:    else if Eq. (35) then
18:       $H_1 \leftarrow 1$  and  $H_3 \leftarrow 0$ 
19:    end if
20:    else if Eq. (34) & Eq. (37) then
21:       $H_3 \leftarrow 1$ 
22:    if Eq. (27) then
23:       $H_2 \leftarrow 1$  and  $H_1 \leftarrow 0$ 
24:    else if Eq. (31) then
25:       $H_1 \leftarrow 1$  and  $H_2 \leftarrow 0$ 
26:    end if
27:    else
28:       $H_1 \leftarrow 0, H_2 \leftarrow 0$ , and  $H_3 \leftarrow 0$ 
29:    end if
30:  end if
31: end for

```

$$\min \sum_{t=t_{st}}^{t_{ed}} \left(E_t^{CESS}(t) - \sum_{h=1}^N E_t^{Dis,H_h}(t) \right) \quad (42)$$

$$E_t^{Grid,H_h}(t) = E_{D,t}^{H_h}(t) - E_t^{Dis,H_h}(t) \quad (43)$$

$$SOC_t^{CESS}(t) = \left(\frac{E_t^{CESS}(t)}{E_{Cap}^{CESS}} \right) \quad (44)$$

where E_t^{Grid,H_h} and E_{Cap}^{CESS} present the energy supplied by the grid and maximum energy stored capacity of CESS. The objective function Eq. (42) is designed to minimize the expected energy from the grid for the entire community while maximizing the use of renewable resources. Algorithm 1 shows the step-by-step procedure for the optimal energy sharing scheme. Moreover, Algorithm 2 illustrates the charging and discharging periods of CESS.

3. Simulation result

In this section, a single simulation is run to demonstrate and qualify the effectiveness of the proposed data-driven and dynamic energy sharing algorithm, as well as to demonstrate

Table 2

Performance analysis of forecasting model.

Performance indicators	H1	H2	H3	PV
MSE (kW)	0.3743	0.4822	0.2135	0.00024
MAE (kW)	0.0131	0.0141	0.0096	0.0086
MAPE (%)	15.882	17.802	15.724	19.783

and qualify the benefits of deploying CESS. The forecasting and optimization algorithm for three homes are simulated on Dell A06 Workstation with 128 GB of memory and Intel(R) Xeon(R) Silver 4210R CPU @ 2.4 GHz processors. The computational time for the optimization algorithm is 5.77s. In the test system, we have considered a grid-connected system where numerous households are taking power from the utility grid and sharing their load with the CESS-integrated PV system. We used energy usage data collected from three homes over 6 months to forecast the energy usage profile of each household. Similarly, forecasted PV generation is calculated using real-time data. For understanding the effectiveness and robustness of the designed data-driven optimization algorithm, the PV power generation and electricity demand for two consecutive days are organized and discretized into 192 15-min intervals.

Table 2 summarizes the performance analysis results of the LSTM model. The prediction results of the model are evaluated by mean square error (MSE), mean absolute error (MAE), and mean absolute percentage error (MAPE). Experimental results show that the error for H_3 is comparatively less than others households. The error value in terms of MSE, MAE, MAPE for the H_3 are .2135 kW, .0096 kW, and 15.724%. Similarly, the prediction errors for PV generation are 2.4×10^{-4} kW, .0086 kW, and 19.783%. Fig. 2 presents the actual and forecasted PV generation and energy consumption profile for two consecutive days. It also shows the results of the data-driven optimization algorithm for the scheduling period of charging and discharging allowance. As shown in the figures, the simulation results cover the days of electricity generation and consumption from November 8, 2020, to November 10, 2020. From Fig. 2, it is observed that the CESS is charged only during the period of power generation while the discharging occurs during the rest of the periods. According to the optimization scheme, two of the houses can draw energy from the battery at the same time because their demand is higher than the rest. As a result, the household with the highest demand can use energy for longer periods. Because of the higher demand, household 3 has been connected to the CESS for a longer period than the others, as shown in Fig. 2(b), (c), and (d). Moreover, household 1 has been allowed for the shortest periods. The allocation of discharging periods has been designed based on the forecasted demand of the individual households.

The battery's SOC is displayed in Fig. 3(a). In this figure, we show the SOC of the battery after the operational periods for each iteration has ended. According to the graph, the discharging allowance at normal conditions keeps the battery from charging during PV power generation. On the contrary,

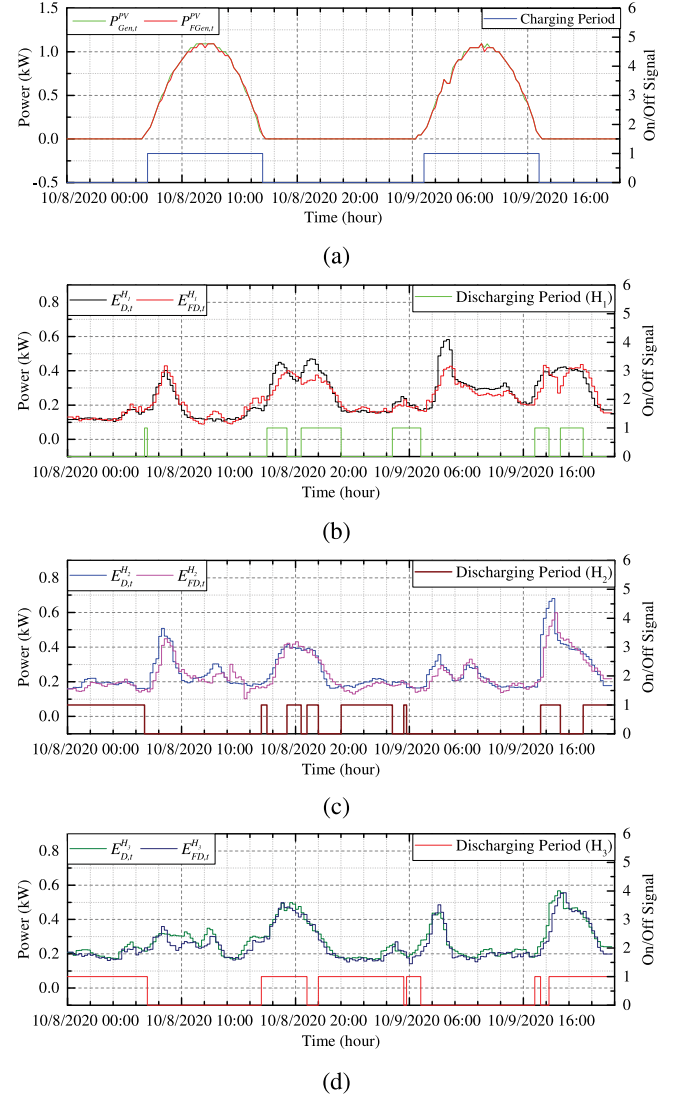


Fig. 2. (a) CESS charging period and CESS discharging periods and energy demand for (b) H_1 , (c) H_2 , and (d) H_3 .

the data-driven optimization algorithm provides a balanced condition between charging and discharging allowance on daily basis. The convergence curve of the proposed scheme is depicted in Fig. 3(b). With the increased use of renewable resources, the proposed optimization process provides an improved method in terms of energy management. The outcome of the proposed objective function is demonstrated in Fig. 4. The volume and the time of utilization of energy, which is stored during PV power generation, are presented in this figure. These diagrams show the energy flow from the grid and energy storage to households under normal and optimized conditions. It has been observed that the battery has supplied less energy to the households under normal conditions, although it contains more energy. Consequently, the households need to take more power from the grid which is responsible for the high electricity bill. However, the use of optimal operation results in greater utilization of energy storage for all households. The figure shows that the battery

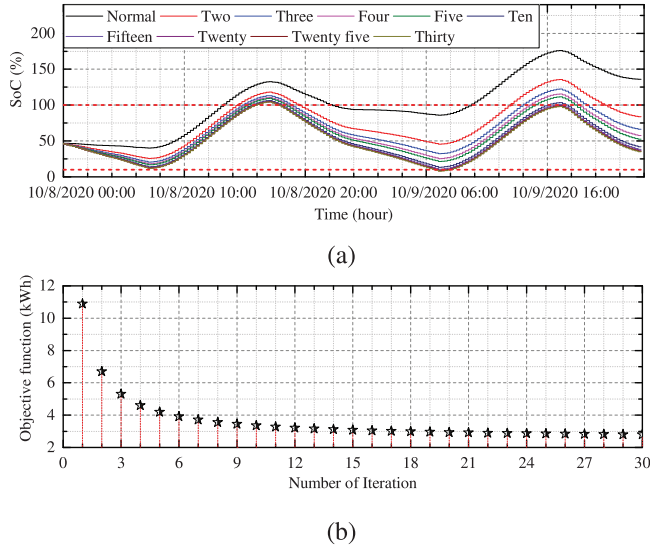


Fig. 3. (a) SOC status of the CESS with iterations and (b) Convergence curve for the proposed optimization algorithm.

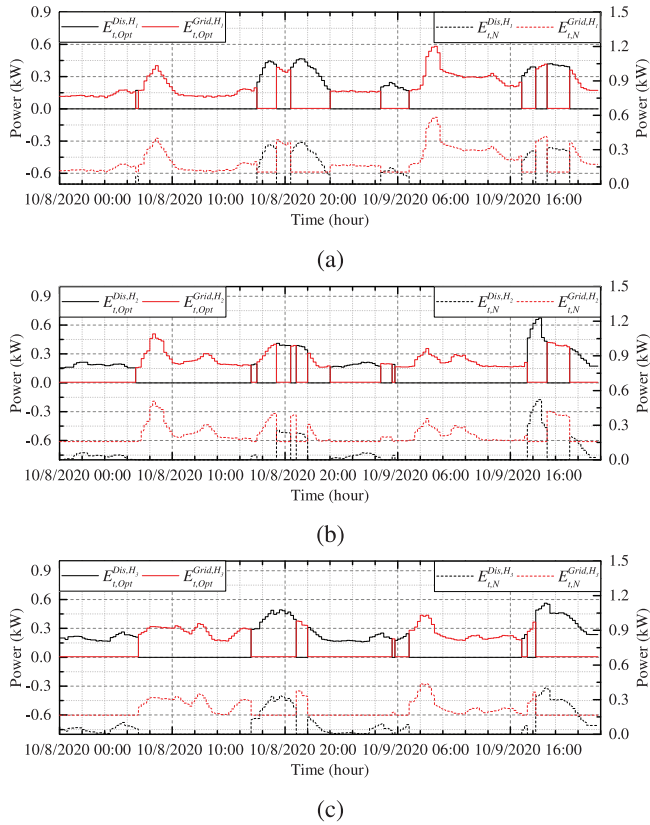


Fig. 4. Grid and CESS energy scenario for (a) H_1 , (b) H_2 , and (c) H_3 .

provides enough energy to each household while remaining within the discharging constraints.

The comparison of the total supplied energy by the grid and battery at normal and optimized condition is presented in Fig. 5. For better perception, the total demand of each household is also included in this figure. Tables 3 and 4 show a summary of energy consumption for each household under

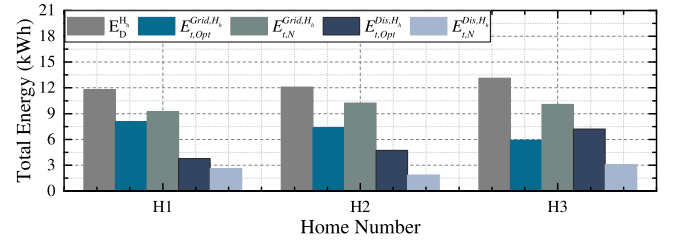


Fig. 5. Energy demand-supply for households.

Table 3

Analysis of the grid and CESS power utilization.

Condition	Normal			Optimal		
House No.	$E_{d,t}^H$	$E_t^{Grid,H}$	$E_t^{Dis,H}$	$E_{d,t}^H$	$E_t^{Grid,H}$	$E_t^{Dis,H}$
H ₁ (kWh)	11.81	9.18	2.62	11.81	8.04	3.76
H ₂ (kWh)	12.09	10.24	1.85	12.09	7.36	4.72
H ₃ (kWh)	13.11	10.07	3.03	13.11	5.91	7.19

Table 4

Analysis of the grid and CESS power utilization.

House No.	H ₁		H ₂		H ₃	
Condition	Nor	Opt	Nor	Opt	Nor	Opt
$E_{d,t}^H$ (kWh)	11.81		12.09		13.11	
$E_t^{Grid,H}$ (%)	77.81	68.13	84.69	60.94	76.83	45.09
$E_t^{Dis,H}$ (%)	22.19	31.86	15.31	39.05	23.16	54.90

normal and optimal conditions. Total electricity demand and percentage of receiving energy from the grid and CESS for each household are also analyzed in this table. Households with a higher and lower energy demand use more and less storage energy, respectively. However, the H_1 and H_3 increase the amount of receiving storage energy approximately to 9.67% and 31.74%. Similarly, the reverse process occurs, while drawing power from the grid.

4. Conclusion

In this study, we generated a structured community energy storage control algorithm based on a predictive model that includes the maximum discharging allowance for each consumer. The proposed predictive model has been achieved lower forecasting error in terms of MAPE of 15.724%. The efficacy of the optimization algorithm is evaluated by the charging–discharging scheduling pattern and the amount of supplying energy of CESS. The proposed system effectively reduces grid energy volume while increasing the use of renewable resources. The greatest improvement is seen in the case of H_3 . Grid energy usage has decreased by 76.83% to 45.09%, while ESS energy usage has increased by 23.16% to 54.90%. Based on the numerical results, it is possible to conclude that the proposed optimization system achieves a reasonable level of performance in the face of the uncertainty and the complexity inherent in community energy storage operations. In the future, a research will be conducted to augment the current approach for comprehensive application through the clustering technique which includes a large number of users and multiple CESS.

CRedit authorship contribution statement

Md. Morshed Alam: Conceptualization, Methodology, Implementation, Writing – original draft, Data curation. **Yeong Min Jang:** Supervision.

Declaration of competing interest

The authors declare that they have no known competing financial interests or personal relationships that could have appeared to influence the work reported in this paper.

References

- [1] IEA, World energy outlook EXECUTIVE SUMMARY, International Energy Agency, Paris, 2019, <https://www.iea.org/reports/world-energy-outlook-2019>.
- [2] Gridflex heeten investigates feasibility of local energy market, 2019, Available from: <https://ict.eu/case/gridflex-heeten-investigates-feasibility-of-local-energy-market/>.
- [3] M. Rawson, E.P. Sanchez, Sacramento municipal utility district PV and smart grid pilot at anatolia, 2013, Sacramento Municipal Utility District.
- [4] B.P. Koirala, E. van Oost, H. van der Windt, Community energy storage: A responsible innovation towards a sustainable energy system? *Appl. Energy* 231 (2018) 570–585.
- [5] Z. Wang, C. Gu, F. Li, P. Bale, H. Sun, Active demand response using shared energy storage for household energy management, *IEEE Trans. Smart Grid* 4 (4) (2013) 1888–1897.
- [6] J. Sardi, N. Mithulananthan, M. Gallagher, D.Q. Hung, Multiple community energy storage planning in distribution networks using a cost-benefit analysis, *Appl. Energy* 190 (2017) 453–463.
- [7] Z. Wang, C. Gu, F. Li, Flexible operation of shared energy storage at households to facilitate PV penetration, *Renew. Energy* 116 (2018) 438–446.
- [8] F. Hafiz, A. Rodrigo de Queiroz, P. Fajri, I. Husain, Energy management and optimal storage sizing for a shared community: A multi-stage stochastic programming approach, *Appl. Energy* 236 (2019) 42–54.
- [9] J. Jo, J. Park, Demand-side management with shared energy storage system in smart grid, *IEEE Trans. Smart Grid* 11 (5) (2020) 4466–4476.
- [10] W. Zhong, K. Xie, Y. Liu, C. Yang, S. Xie, Multi-resource allocation of shared energy storage: A distributed combinatorial auction approach, *IEEE Trans. Smart Grid* 11 (5) (2020) 4105–4115.
- [11] R. Carli, M. Dotoli, J. Jantzen, M. Kristensen, S. Ben Othman, Energy scheduling of a smart microgrid with shared photovoltaic panels and storage: The case of the ballen marina in samsø, *Energy (Oxf.)* 198 (117188) (2020) 117188.
- [12] L. Sun, J. Qiu, X. Han, X. Yin, Z.Y. Dong, Capacity and energy sharing platform with hybrid energy storage system: An example of hospitality industry, *Appl. Energy* 280 (115897) (2020) 115897.
- [13] P. Scarabaggio, R. Carli, J. Jantzen, M. Dotoli, Stochastic model predictive control of community energy storage under high renewable penetration, in: 29th Mediterranean Conference on Control and Automation, MED, 2021.
- [14] Z. Li, C. Zang, P. Zeng, H. Yu, H. Li, Two-stage stochastic programming-based model predictive control strategy for microgrid energy management under uncertainties, in: International Conference on Probabilistic Methods Applied to Power Systems, PMAPS, 2016.
- [15] H. Zhuang, Z. Tang, J. Zhang, Two-stage energy management for energy storage system by using stochastic model predictive control approach, *Front. Energy Res.* 9 (2021).
- [16] M.A. Hossain, R.K. Chakraborty, M.J. Ryan, H.R. Pota, Energy management of community energy storage in grid-connected microgrid under uncertain real-time prices, *Sustain. Cities Soc.* 66 (102658) (2021) 102658.
- [17] M.M.U. Rashid, et al., Home energy management for community microgrids using optimal power sharing algorithm, *Energies* 14 (4) (2021) 1060.
- [18] K.G. Di Santo, S.G. Di Santo, R.M. Monaro, M.A. Saidel, Active demand side management for households in smart grids using optimization and artificial intelligence, *Measurement (Lond.)* 115 (2018) 152–161.
- [19] M. Hemmati, B. Mohammadi-Ivatloo, M. Abapour, A. Anvari-Moghaddam, Day-ahead profit-based reconfigurable microgrid scheduling considering uncertain renewable generation and load demand in the presence of energy storage, *J. Energy Storage* 28 (101161) (2020) 101161.
- [20] A. Bouakkaz, A.J.G. Mena, S. Haddad, M.L. Ferrari, Efficient energy scheduling considering cost reduction and energy saving in hybrid energy system with energy storage, *J. Energy Storage* 33 (101887) (2021) 101887.
- [21] M.M. Alam, M.O. Ali, M. Shahjalal, B. Chung, Y.M. Jang, Optimal energy management among multiple households with integrated shared energy storage system (ESS), in: Proc. International Conference on Ubiquitous and Future Networks, ICUFN, 2021, pp. 399–404.
- [22] Y. LeCun, Y. Bengio, G. Hinton, Deep learning, *Nature* 521 (7553) (2015) 436–444.